

Temporal variations of coda Q : an attenuation-coefficient view

Igor B. Morozov

Department of Geological Sciences, University of Saskatchewan, Saskatoon, SK S7N 5E2 Canada

Igor.Morozov@usask.ca

Abstract

During the past 30 years, numerous studies addressed the spatial and temporal variations of coda wave attenuation, and particularly in relation to major earthquakes and volcanic eruptions. Both the coda quality factor, Q_c , and its frequency dependence are often found to change prior and following such events, which is usually attributed to changes in scattering properties of the subsurface. However, Q_c is also strongly sensitive to the assumed theoretical models, which are usually insufficiently accurate for constraining the actual relationships between the geometrical spreading, anelastic dissipation, and scattering. This inaccuracy often leads to significant exaggeration of the attenuation effects, and particularly scattering. To resolve this problem, a phenomenological approach is proposed using the temporal attenuation-coefficient, $\chi(f)$ instead of $Q(f)$. Coda-wave and other attenuation case studies suggest that $\chi(f)$ typically linearly depends on f , with both the intercept $\gamma = \chi(0)$ and slope $d\chi(f)/df = \pi Q_e^{-1}$ being sensitive to the physical state of the subsurface. Two published examples of temporal variations of local-earthquake coda Q are revisited: non-volcanic (Stone Canyon in central California) and volcanic (Mt. St. Helens, Washington). In both cases, such linear $\chi(f)$ patterns are found, and the effects of geometrical spreading (γ) on coda attenuation are

significantly stronger than those of Q_e^{-1} . At Stone Canyon, γ values ranged from 0.035 to 0.06 s^{-1} and Q_e varies from 3000 to 10000, with γ increasing and Q_e decreasing during the winter season. At Mt. St. Helens, $\gamma \approx 0.18 \text{ s}^{-1}$, and Q_e changed from 400 before the eruption to 750 after it. The observed temporal variations can be explained by near-surface effects (seasonal variations in the non-volcanic case and magma- and geothermal-system related in the volcanic case). Scattering-attenuation does not appear to be a significant factor in these areas, or otherwise it may be indistinguishable from the intrinsic attenuation in the data.

Introduction

Measurements of seismic coda attenuation provide critical information about the physical state of the Earth's interior. Due to its averaging over multiple wave types and significant volumes of the lithosphere, coda provides good stability of estimates and allows detection of small temporal variations in attenuation related to volcanic activity or environmental changes. However, the association of the measured quantity (which is usually the frequency-dependent apparent coda "quality" factor, Q_c) to the in-situ physical properties is still not straightforward and may be prone of pitfalls and uncertainties. Despite its well-known apparent character (e.g., Aki, 1980), Q_c is conventionally interpreted directly in terms of scattering scale-lengths and r.m.s. velocity fluctuations (e.g., Jin and Aki, 1986). Such interpretation is usually based on the single-scattering model (Aki and Chouet, 1975) or on its extensions to multiple scattering (e.g., Dainty and Toksöz, 1977; Fehler et al., 1992). All of these models use a number of strong assumptions, such as the uniform velocity background, perfectly-known geometrical

spreading (GS), absence of free-surface effects and lithospheric reflectivity, and isotropic and often uniformly-distributed scattering. However, these assumptions are insufficiently accurate in most observational situations, and their inaccuracy may account for the entire frequency dependence of Q_c and lead to strong (up to 20-30 times) difference between the apparent and the in-situ Q^{-1} in many observations (Morozov, 2008, 2009a, b).

Sensitivity of the frequency-dependent Q_c (as well as of Q in general) to GS corrections is well-known (e.g., Kinoshita, 1994). Broad acceptance of standard reference models for GS, such as $G(t) = t^{-1}$ for local-earthquake body waves (here and below, t is the travel time, and f is the frequency) allows comparisons between the $Q_c(f)$ models derived for different areas or time intervals; however, this abstract reference reduces these $Q_c(f)$ curves back to descriptions of the coda amplitudes and not necessarily of the Earth's attenuation properties. For an unbiased interpretation of the in-situ Q , measurements should be conducted so that the results are independent of GS variations.

Recently, I suggested that the uncertainties due to the GS- $Q(f)$ trade-off can be removed if instead of using the quality factor $Q(f)$, we return to interpreting the temporal attenuation coefficient, $\chi(f)$ (denoted $\alpha(f)$ in Morozov 2008). This attenuation coefficient incorporates the variations of GS and is directly measured in most observations. It can also be modeled numerically (Morozov et al., 2008) and correlated to geological structures and tectonic ages. The trade-off and sensitivity to GS assumptions are introduced by the commonly employed transformation $Q(f) = \pi f / \chi(f)$, which also leads to Q increasing with frequency (up to $Q \propto f$) when the zero-frequency limit of $\chi(f)$ is non-zero and positive (Morozov, 2009a). From a worldwide data compilation (Morozov

2008), $\chi(0)$ is indeed positive for crustal body, surface, and coda waves.

In all cases I considered so far (Morozov 2008, 2009a, in press, and in review) the use of $\chi(f)$ simplified the interpretation and revealed data relationships that would be hard to notice in the apparent $Q(f)$ form. Most importantly, $\chi(f)$ typically shows linear dependencies on f , which allow its presentation in the form of $\chi(f) = \gamma + \pi f / Q_e$, where $\gamma = \chi(0)$ can be interpreted as the residual GS, and Q_e represents the “effective attenuation” (Morozov, 2008). Because of their natural connection to the observable $\chi(f)$, coordinates (γ, Q_e) often lead to broader and clearer separation between different observations than parameters (Q_0, η) of the commonly-used $Q(f) = Q_0 f^\eta$ power law.

In this paper, I briefly introduce the $\chi(f)$ concept and then use it to revisit two observations of temporal variations of local-earthquake coda attenuation. Many observations of coda attenuation (Q_c) varying over time scales from several weeks to a few years were made, such as by Chouet (1979), Aki (1980), Stewart et al. (1983), Rhea (1984), Novelo-Casanova et al. (1985), Sato (1986), Jin and Aki (1986), Peng et al., 1986, Sato, 1986; and Gusev (1997). The results were invariably interpreted according to Aki’s (1969) coda-scattering model, i.e. by attributing the entire effect to the variations of in-situ Q , and consequently to crustal heterogeneity and dissipation. Whereas not all of these observations are equally convincing, the very first of them (Chouet, 1979; Aki, 1980) presented a spectacular Q_c variation recorded continuously over about a year of an extensive aftershock study in central California. This study was also sufficiently detailed and well-documented in order to attempt reproducing a part of its $\chi(f)$ data in this paper.

Re-examination of the published Stone Canyon data shows that the $\chi(f)$ picture

offers different, simpler perspectives on the observed temporal variation. As shown below, $\chi(f)$ retains its linear character during the different periods of observations, with both γ and Q values changing with time. Contrary to what is commonly assumed, Q^{-1} plays a relatively minor role in the observed coda, and it is responsible for only about one third of its attenuation at the highest frequencies. The main effect, including the observed temporal variation of the apparent Q_c , belongs to γ , i.e., to the velocity structure. Realization of this fact leads us to emphasizing the near-surface effects, by contrast to the very strong (several per cent of r.m.s. velocity fluctuations), rapid (within a week), yet enigmatic variations of velocity heterogeneity within a large volume (tens of kilometres radius) of the lithosphere suggested by Aki (1980).

In many studies, temporal variations of coda Q_c were studied at volcanoes (e.g., Chouet, 1976; Fehler et al., 1988; Londono, 1996; Moncayo et al., 2004, Novelo-Casanova et al., 2006; Del Pezzo et al. 2004). In these cases, the key observed coda characteristics usually are the temporal variations of the values of Q_c at selected frequencies and also the dependences of Q_c on frequency. By contrast to non-volcanic regions where strong frequency dependences are common ($\eta \approx 1$; e.g., Roecker et al. 1982), volcanic Q_c often varies from weak (Chouet, 1976; Fehler et al., 1988) to strong frequency-dependences (e.g., Londono, 1996; Moncayo et al., 2004). No widely accepted theory exists to explain this variation, and particularly the weak frequency dependence of Q_c at volcanoes. Aki (1980) suggested that in the presence of magma, the intrinsic attenuation could be predominant and leading to a frequency-independent within the seismic band Q^{-1} , whereas scattering should generally cause Q^{-1} to decrease with increasing frequency (Dainty, 1981). Roecker et al. (1982) also suggested that Q_c strongly

depends on the depth of sampling by scattered waves, which was inferred from coda lag times.

However, note that the above contrasting of scattering- to intrinsic- Q and frequency-independent to frequency-dependent Q_c relies entirely on the selected theoretical model, for which the single-scattering model (Aki and Chouet, 1975) is used in most cases. Although giving a convenient framework for comparing the observations by reducing them to $Q_c(f)$, this model is based on so strongly simplified assumptions that it leads to a fairly distorted physical picture of coda attenuation. In this picture, the residual GS is presented as an enigmatic frequency-dependence of Q_c , Q^{-1} may be significantly over-estimated, the significance of scattering is exaggerated, and scatterers themselves are broadly distributed within the lithosphere instead of (maybe) being concentrated closer to the surface or fault zones as the geology usually suggests (Morozov, 2008, 2009a, b). This picture should be particularly problematic in volcanic studies, where contrasting surface topography and extreme subsurface heterogeneity are abundant.

Unfortunately, in the conventional practice, such reliance on a grossly inaccurate model affects not only interpretation but even the initial data presentation. Attenuation data are typically shown in the form of Q_c , which is obtained by dividing the log-amplitude data by the theoretical GS prediction. It appears that simply by switching back to the phenomenological attenuation coefficient $\chi_c(f) = \pi f / Q_c(f)$, the model-related GS artefact can be “undone,” and comparison of the observed coda properties becomes reliable.

The results of this simple transformation are quite impressive. Even by using published datasets, this approach leads to several revealing observations that are not

visible in the $Q_c(f)$ view. To illustrate this approach, I briefly revisit the data from Mount St. Helens eruption by Fehler et al. (1988). Similarly to the study by Chouet (1979), this dataset also contains clear (but different) temporal and frequency-dependent effects, allows comparing the GS and Q^{-1} contributions, and leads to interesting observations of their variations during the process of volcanic activity.

Attenuation coefficient and Q

In a “reasonably,” but still imperfectly known Earth structure, the source-, receiver-, and GS-corrected path contribution to the seismic amplitude can be written as

$$\delta P(f, t) = \exp\left[-\chi^*(f, t)\right], \quad (1)$$

with only the normalization condition $\chi^*(f, t=0) = 0$ imposed on the exponent χ^* . Further, for attenuation measurements involving relatively short time lags, $\chi^*(f, t)$ can be considered as approximately proportional to t :

$$\chi^*(f, t) = \chi(f)t. \quad (2)$$

This is the standard perturbation- (or scattering-) theory approximation, which retains the first-order term in the Taylor series for $\ln\delta P(f, t)$ in respect to t . I will refer to both quantities χ^* and χ in eqs. (1-2) as the generalized attenuation coefficients, which combine the effects of the variable or inaccurately compensated GS with the elastic and anelastic attenuation losses. Note that χ was denoted ‘ α ’ in Morozov (2008, 2009a), but here I change the notation in order to avoid collision with the spatial attenuation coefficient used in Aki and Richards (2002).

Denoting the frequency-independent part of χ by $\gamma = \chi(0)$, we have:

$$\chi(f) = \gamma + \frac{\pi}{Q_e} f, \quad (3)$$

where Q_e is the “effective attenuation” quality factor, and γ describes the residual GS (note that γ is measured in frequency units). Such interpretation of these parameters is based on the assumption that the residual GS is frequency-independent. This assumption is natural for common frequency-independent GS models, and it is much less restrictive than the conventional assumption of $\gamma = 0$. In cases when the background GS is frequency-dependent (for example, in Pn studies), this assumption may be questionable, and then the differentiation of the residual GS from Q^{-1} appears unfeasible. Nevertheless, even in such cases, the $\chi(f)$ description remains consistent without separation of the GS and attenuation terms (Morozov, in press). Note that from eq. (3) the effective attenuation Q_e may be frequency-dependent; however, such dependence was not observed in all observations that I considered so far (Morozov, 2008, in press, in review, and also in this paper).

In the conventional approach (Aki and Chouet, 1975), the attenuation coefficient $\chi(f)$ is replaced with a new parameter

$$Q(f) = \frac{\pi f}{\chi(f)}, \quad (4)$$

and the interpretation is carried out strictly in its terms. From the general expression (3), we therefore have:

$$Q^{-1}(f) = Q_e^{-1} + \frac{\gamma}{\pi f}. \quad (5)$$

With $Q_e = \text{const}$, this formula was used by Dainty (1981) to describe the S -wave $Q^{-1}(f)$ at 1 - 30 Hz. Note that representing the r.h.s. of eq. (4) as Q is motivated by expecting that $\chi(f) \rightarrow 0$ when $f \rightarrow 0$. This is correct in a boundless and uniform space, in which the GS is accurately known and can be considered as completely corrected for in eq. (1). In such a case, Q is equal to the in situ $Q_{\text{in-situ}}$, and in the absence of attenuation ($Q_{\text{in-situ}}^{-1} = 0$), $\ln \delta P(f, t) = 1$. However, if such a medium also has an unaccounted-for velocity or reflectivity structure causing $\gamma \neq 0$, then Q in eq. (4) would exhibit a spurious dependence on frequency. For example, when $\gamma > 0$, the apparent (observed) Q would linearly increase with frequency. Such behaviour is often observed for crustal body and coda waves, for which $\gamma \approx 0.01 - 0.08 \text{ s}^{-1}$ (Morozov, 2008). In the examples below, γ ranges from ~ 0.04 to 0.2 s^{-1} .

As shown in eq. (4), the $Q(f)$ description can be viewed as a special case of the attenuation coefficient (3). By definition of its parameters, this special case is designed to only work with perfectly-compensated GS, and this limitation causes most problems of this description. In the presence of variable residual GS (which is actually the common case), the general $\chi(f)$ form appears to be most suitable and less prone to uncertainties.

Q_e is a different property compared to the conventional $Q(f)$, and therefore its measurement procedure is also different. In fact, $Q(f)$ only represents the $\chi(f)$ itself, i.e. the logarithm of the residual wave amplitude remaining after selected source-, receiver-, and GS corrections at a fixed frequency. By contrast, Q_e correlates the values of $\chi(f)$ at different frequencies, i.e., it describes the $\chi(f)$ scaling law with frequency. Although this property usually turns out to be quite simple, it is difficult to discern in the $Q(f)$ form.

In consequence of its different nature, the resulting values of Q_e are also usually significantly different from $Q(f)$. As illustrated in Morozov (2008 and in press), for various types of crustal waves, γ is usually positive, and Q_e is higher than the largest $Q(f)$ observed. In many cases of strong frequency dependence of $Q(f)$ ($\eta > 0$), Q_e is 20 - 30 times higher than Q_0 . This contrast is particularly strong in areas with greater residual GS (γ) and in studies conducted at lower frequencies (Morozov, 2008). This shows that the attenuation related to anelastic energy dissipation and scattering is often significantly weaker than it may appear from the value of Q_0 or even from $Q(f)$ at the highest measured frequency. This observation will be illustrated in the examples below.

According to eq. (3), the critical step in interpreting the $\chi(f)$ dependences consists in their plotting in linear frequency scales and establishing their linearity (or non-linearity) with frequency. Unfortunately, this simple analysis is practically never performed in attenuation studies. In the following application to local-coda data, I will try using the attenuation-coefficient (3) dependences to answer four questions: 1) whether they can be considered linear in f , 2) if so, whether non-zero intercept values $\gamma = \chi(0)$ are indicated by the data, and 3) whether both γ and Q_e depend on the times of observations, and 4) what these variations suggest about the temporal variations and spatial distributions of GS and Q^{-1} within the subsurface.

Temporal variations of local-earthquake coda $Q(f)$

To illustrate the relation of $Q(f)$ -type models to $\chi(f)$, let us review the data from an aftershock study of an earthquake swarm along the San Andreas Fault (SAF) in central California. From July 17, 1973 to June 24, 1974, 185 earthquakes of magnitudes 0.9 to

3.3 were recorded at the temporary station STC located in Stone Canyon, approximately 1 km west of the SAF (Chouet, 1979). Note that the presence of such major, linear crustal structure as the SAF zone in addition to the sedimentary and crustal layering makes this area particularly interesting for studying the effects of GS on attenuation measurements.

Figure 1a reproduces the frequency-dependent $Q^{-1}(f)$ available from Aki (1980). The observations were grouped into four time intervals: 7/18/1973 – 9/11/1973 (STC-1), 9/12/1973 – 11/10/1973 (STC-2), 11/11/1973 – 2/10/1974 (STC-3), and 2/11/1974 – 6/24/1974 (STC-4). From these data, $Q^{-1}(f)$ clearly increased at all frequencies sometime from mid-September to mid-October 1973 (Aki, 1980). However, beyond this general observation, more detailed variations of attenuation are difficult to analyze from this plot. Chouet (1979) and Aki (1980) described this change as intriguing but unclear, and broadly attributed it to some rapid but strong variations of lithospheric heterogeneity within a large volume (tens of kilometres radius) of the lithosphere.

However, re-plotting the same data in terms of $\chi(f) = \pi f Q^{-1}(f)$ reveals linear attenuation patterns showing the detailed relationships between the datasets (Figure 1b). It shows that the convergence of all $Q^{-1}(f)$ near ~25 Hz (Figure 1a) is incidental and principally related to dividing the values of attenuation coefficients $\chi(f)$ by the frequency. By contrast, comparison of the intercepts and slopes of the attenuation coefficient trends (dashed lines in Figure 1b), shows that: 1) GS factors are slightly below $\gamma \approx 0.04 \text{ s}^{-1}$ for STC-1 and about $0.05 - 0.06 \text{ s}^{-1}$ for STC-2 through STC-4; 2) attenuation factor values are high, with $Q_e \approx 10000$ for STC-1 dropping to $Q_e \approx 3000 - 4500$ for STC-2 through STC-4. Such high γ values appear characteristic for central California (Morozov, in press)

and may be related to the proximity of the SAF. At the same time, the values of Q_e appear unusually high (the previously observed value was $Q_e \approx 1250$; Morozov, in press), which may indicate a well-consolidated crust in the Stone Canyon area.

The observed linear $\chi(f)$ dependences are reasonable within roughly estimated 10% error on χ (Figure 1b, inset). Unfortunately, full estimation of errors in $\chi(f)$ measurements requires revisiting the raw amplitude data, which is not available in this study. Chouet (1979) reported errors in $Q(f)$ at $\sim 1 - 3\%$ levels, which are similar to error estimates in many other studies. However, these values only correspond to measuring the time-domain slopes of the logarithms of narrow-band pass filtered r.m.s. amplitudes across long (~ 30 -sec) time intervals. Such slopes are well-constrained and indeed may have small errors; however, these errors only refer to measuring the time decay of amplitude recorded at a given point and at a fixed frequency. These values may still be affected by the spatial and frequency amplitude variations (e.g., resonances, tuning), which are apparent from the systematic amplitude variations in Figure 1b. Note the “spectral scalloping” resulting in reduced amplitudes at 1.5, 6 (with one exception for STC-1), and 24 Hz and increased at 3 and 12 Hz in all recordings (Figure 1b). Because of such amplitude variations, the scatter of the resulting $Q(f)$ is typically much stronger than expected from Aki’s (1969) model with such low $Q(f)$ errors (see Figure 3).

The uncertainties in the resulting (γ, Q_e) values can be examined by using the standard linear regression analysis. Figure 2 shows cross-plots of (γ, Q_e) for the four time intervals, with their optimal parameter values shown by diamonds and areas of likelihood levels above e^{-2} contoured. The stronger amplitude oscillations at lower frequencies

(Figure 1b) cause the most of the errors for STC-1 and STC-2 periods (Figure 2a), and by excluding these frequencies, significantly tighter estimates of γ and Q_e can be obtained (Figure 2b). However, dropping the single 1.5-Hz reading for STC-1 shows that its Q_e^{-1} can in fact be set equal 0 (Figure 2b), which means that the attenuation in this interval may be too low to be detectable.

With either using the frequencies below 6 Hz or not, the variations of attenuation parameters with observation time are clear and well-constrained (Figure 2). The attenuation increases from STC-1 to STC-3 and then reduces to STC-4. However, the contribution of γ dominates that of Q_e even at the largest observation frequency (i.e., $\gamma > \pi f / Q_e$ with $f = 24$ Hz; Figures 1b and 3). For example, for STC-2, the GS and Q_e^{-1} contributions would only become equal at the “cross-over” frequency $f_c = \gamma Q_e / \pi \approx 86$ Hz, which is far above the observation band. Thus, it appears that the “geometrical” effect should be the main cause of both the apparent coda Q_c attenuation and of its temporal variation.

By comparing the temporal trends of γ and Q_e to the $\chi(f)$ data derived from $Q(f)$ for $f = 24$ Hz shown by Chouet (1979), we can further evaluate the significance of these trends. Despite their wide scatter, the individual χ_c data are consistent with the inferred temporal trends. Notably, there actually appears to be no increase in χ_c until the start of the rain season (October 7, 1973; Figure 3). Therefore, contrary to the conclusion by Aki (1980), it is still likely that the increase of both γ and Q_e^{-1} was associated with a change in the near-surface conditions caused by the rain and rising water table.

Four significant differences of our empirical $\chi(f)$ model compared to Aki’s (1969)

coda scattering model allow us to look for the source of coda in the near subsurface. First, as determined above, the GS factor γ (and not scattering) dominates the coda attenuation at Stone Canyon. GS is most sensitive to the near-surface structure, where the strongest velocity contrasts and reflectivity are present. Numerical waveform coda modeling (Morozov et al., 2008) showed that introduction of a low-velocity, high-attenuation layer in the upper crust can significantly increase γ , and therefore the effect of rising water table could be qualitatively consistent with the observed increase of γ (Figure 3). Second, in our model, values of Q_e are significantly higher (3000 - 10000 compared to 100 - 1000 by Chouet, 1979), and this smaller amount of attenuation could therefore be attributed to the upper crust. Third, the attenuation (Q_e^{-1}) is frequency-independent, and therefore it does not have to be explained by scattering but could be caused by anelastic losses (e.g., due to fluid viscosity in wet weathered near-surface layers). Finally, another possibility for variable Q_e is that similarly to Q_c , this quantity may be related not only to the crustal attenuation, but also to the spatial variations of scattering amplitudes. This factor is also likely to be most pronounced in the uppermost parts of the crust and sensitive to precipitation, and it will be further discussed in *Discussion*.

Temporal change in coda attenuation during Mount St. Helens eruption

Another interesting example of temporal variations of coda attenuation was given by Fehler et al. (1988). Three groups of measurements were conducted at Mt. St. Helens: prior to the September 3-6, 1981 eruption, during the eruption, and after it. In the coda quality-factor form, the attenuation (Q_c^{-1}) relatively weakly varied with frequency within

each of these intervals and decreased by 20 - 30% after the eruption (Figure 4a). Fehler et al., (1988) also noted the attenuation peak near 10 Hz, which may correspond to the peak at 0.5 Hz hypothesized by Aki (1980) for non-volcanic regions. Aki (1980) interpreted this peak as caused by scattering and estimated the corresponding scale-length of lithospheric heterogeneity to be ~4km. Following the same argument, Fehler et al. (1988) suggested that a heterogeneity scale-length of ~500 m could be responsible for the 10-Hz Q_c^{-1} peak at Mount St. Helens.

However, if we do not assume scattering from the very beginning but re-plot the same data in the $\chi_c(f) = fQ_c^{-1}(f)$ form, a different interpretation is revealed (Figure 4b). Above ~18 Hz, $\chi_c(f)$ shows linear patterns similar to those in Figure 1. Their intercept values $\gamma \approx 0.18 \text{ s}^{-1}$ are 3 - 4 times higher than those in Figure 1, likely because of the stronger positive GS (defocusing) caused by the cone of the volcano. Similarly to the case of Figure 1 (but somewhat less dramatically), the effect of the “true” attenuation (Q_e^{-1}) represents only about a half of the observed coda attenuation, and the rest is represented by the residual GS. The peak in the apparent Q_c^{-1} near 10 Hz likely corresponds to a transition from predominantly surface waves constituting the coda below ~15 Hz to mostly body waves above this frequency. Such different coda waves would require different GS corrections, and when a single correction is used, they lead to an apparent “absorption band” (Morozov, 2008). Surface waves may have negative GS intercept values (Morozov, 2009a, and in review), which can be noted by extrapolating the $\chi_c(f)$ trends below 6 - 10 Hz frequencies (Figure 4b).

Interestingly, the pre-eruption GS value of $\gamma \approx 0.18 \text{ s}^{-1}$ increased to $\sim 0.25 \text{ s}^{-1}$

during the eruption and returned to its original value afterwards (dashed grey lines in Figure 4b). The return to its original value could be expected, because γ is a property of the structure (shape of the mountain and its subsurface), which generally returned to its original state. The co-eruptive increase of γ was likely related to the inflation of the cone of the volcano (Dzurisin et al., 1981). Attenuation decreased from $Q_e \approx 400$ before the eruption to ~ 750 after it (Figure 4b). This change could be explained by the removal of magma from the volcano chambers and reduction of anelastic attenuation. Note that this is a significantly stronger change (about 50%) compared to the 20-30% change in the apparent $Q_c^{-1}(f)$. At the same time, the values of Q_e are about twice higher than those of Q_c (Figure 4b), and therefore a smaller volume of attenuative material needs to be removed in order to account for this change.

The character of the co-eruptive $\chi_c(f)$ curve in Figure 4b is less clear, suggesting an increase in both γ (which is likely true to some extent, due to cone inflation) and Q_e to ~ 1400 (which is likely too high for this area). Two possible reasons could lead to the increased values of both of these parameters: 1) migration of the earthquake sources to the top of the mountain during the eruption, and 2) increased high-frequency noise during the eruption, causing over-estimated Q_c values. This second reason appears quite likely, judging by the near-constant $\chi_c(f)$ values at 20 -40 Hz during the eruption (Figure 4b). These and other explanations could be examined further by revising the raw data and by modeling, which is, however, outside of the scope of this paper.

Discussion

The above analysis shows that the temporal attenuation coefficient $\chi(f)$ contains

more information than usually recovered by converting it into the conventional $Q(f)$ form. Attenuation-coefficient plots allow grouping the observed dependences into consistent (often linear) patterns and provide wider and clearer separations between responses from different structures. Parameters of such responses can be measured quantitatively and irrespectively to the uncertainties of the assumed GS and theoretical models. The resulting measurement reveal more detail in the attenuation patterns, and allow detecting temporal trends in GS and Q variations that were not noticed before.

Scattering certainly represents the main mechanism of seismic coda generation; however, this still does not mean that it is also responsible for all coda properties. Before the observed coda amplitudes can be interpreted in terms of scatterers' parameters (i.e., scale-lengths, opening and closing of micro-cracks, etc.), the following factors need to be accounted for: 1) 3D structure and experiment geometry, including the major reflecting boundaries, free-surface topography, sedimentary layering, and fault zones; 2) bending and reflecting rays, variations of reflection amplitudes with incidence angles, and tuning effects; 3) intrinsic attenuation, and 4) source and receiver directivity. In real-Earth problems and at seismological frequencies, these factors are undoubtedly of superior order compared to elastic scattering on random, small-scale heterogeneities. If scattering is still required after these factors are accounted for, then the next critical factors are: 5) spatial distribution of scatterers, and 6) their magnitudes and scale-lengths. Clearly, in a model-based approach, factors 1) - 5) are practically intractable with the existing datasets and limited knowledge of the lithospheric structure; however, this still does not mean that they can be ignored and a uniform-space, isotropic scattering model considered instead.

Despite the difficulties of the model-based approach, attenuation data can be easily interpreted phenomenologically, as described in this paper and in Morozov (2008). The attenuation coefficient χ is measured directly from the data, and if linear $\chi(f)$ segments are found, they represent strong indications of wave types that are stable within the corresponding frequency intervals. Within the usual measurement uncertainties, factors 1)-2) and 4) become cumulatively described by the empirical GS, such as parameter γ used in this study. The effective attenuation and its frequency dependence can then be measured from the slope and curvature of $\chi(f)$, respectively. Unfortunately, it appears that after the residual empirical GS is measured, differentiation between scattering and intrinsic attenuation becomes impractical in real measurements (Morozov, 2008, in press).

It is known (e.g., Aki, 1980) that the frequency-dependent Q_c measured in conventional measurements is an apparent quantity which essentially only gives a standard form for representing the time-domain coda shapes. Interpretation of this quantity in terms of physical parameters of the medium (such as temperature, pressure, fluids, crack density) needs to be done with caution, because Q_c may not relate to attenuation or even to any other local property of the medium. In our examples (Figures 1 and 4a), Q_c was mostly caused by the residual GS, which also appeared to be the case in many observations of strongly frequency-dependent Q (Morozov, 2008 and in press).

Q_e is also an “apparent” property that still needs to be inverted for the local physical parameters of the medium. Nevertheless, frequency-independence of Q_e observed in many examples gives a strong support to its being actually related to the intrinsic Q of the medium. This can be seen from the symmetry with which we treat the residual GS and

Q^{-1} in our $\chi(f)$ approach. Generally, if frequency-dependence allows us to separate the GS- and Q^{-1} - related contributions in the observed coda decay rates (3), then the same decomposition could be applied to the corresponding in-situ properties. Consider the following expression for the observed path factor:

$$P(t, f) = G_0(t, f)e^{-\chi^* t}, \quad (6)$$

where $G_0(t, f)$ is the theoretical GS factor (for example, $t^{-\nu}$) and χ^* is given in eq. (2).

Conventionally, (i.e., assuming that there is no GS contribution in it), χ^* is attributed to the in-situ Q^{-1} along the “wave path” (e.g., Der and Lees, 1985):

$$\chi^* = \pi f t^* = \pi f \int_{path} Q^{-1} d\tau, \quad (7)$$

where τ is the time within the travel path measured from 0 to t . However, note that with inaccurate $G_0(t, f)$, the exponent in path correction (6) is not guaranteed to be proportional to f , and therefore we need to return to equation to eq. (2) and generalize the path-average formula (7) as $\chi^* = \chi t$, with

$$\chi = \frac{1}{t} \int_{path} \chi_i d\tau, \quad (8)$$

and χ_i being the “intrinsic” differential attenuation coefficient. Thus, in its use and meaning, $\chi(f)$ is quite similar to the traditional fQ^{-1} , in the sense that it can be averaged over wave paths to predict corrections to the logarithms of seismic amplitudes. Similarly to eq. (3), it can be decomposed into frequency-independent and dependent parts:

$$\chi_i(f) = \gamma_i + \frac{\pi}{Q_i} f, \quad (9)$$

which can be interpreted as the local GS density (γ_i) and intrinsic/scattering attenuation (Q_i^{-1}), respectively, so that:

$$\gamma = \frac{1}{t} \int_{path} \gamma_i d\tau, \text{ and } Q_e^{-1} = \frac{1}{t} \int_{path} Q_i^{-1} d\tau. \quad (10)$$

Note that from our observations above, the largest and time-dependent values of both γ_i and Q_i^{-1} should be concentrated in the near surface and/or in the area of the volcanic magma chambers and hydrothermal systems.

Conclusions

By using the temporal attenuation-coefficient $\chi(f)$ description instead of the conventional frequency-dependent Q , observations of coda attenuation can be systematically analysed without the ambiguities of simplified scattering models. Analysis of coda and other Q case studies shows that $\chi(f)$ typically linearly depends on f , with both the intercept $\gamma = \chi(0)$ and slope $d\chi(f)/df = \pi Q_e^{-1}$ varying with changing observation conditions.

Two examples of temporal variations of local-earthquake coda Q_c were considered: non-volcanic (Stone Canyon in central California) and volcanic (Mt. St. Helens, Washington). In both cases, the effects of geometrical spreading (γ) on coda attenuation are stronger than those of Q^{-1} . At Stone Canyon, γ values range from 0.035 to 0.06 s⁻¹ and Q_e varies from 3000 to 10000, with γ increasing and Q_e decreasing during the

winter. At Mt. St. Helens, $\gamma \approx 0.18 \text{ s}^{-1}$, and Q_e varies from 400 before the eruption to 750 after it. The observed temporal variations can be explained by near-surface effects (seasonal variations in the non-volcanic case and magma- and geothermal-system related in the volcanic case). The effects of Q^{-1} are also much weaker ($Q_e^{-1} \ll Q_c^{-1}$) than those expected by directly attributing the Q_c values to the subsurface. Scattering-attenuation does not appear to be a significant factor in these areas, or at least it is indistinguishable from the intrinsic attenuation in the data.

Acknowledgments

This study was supported by NSERC Discovery Grant RGPIN261610-03. GNU Octave software (Octave, 2009) was used for computations, and GMT programs (Wessel and Smith, 1995) - for preparation of illustrations.

References

- Aki, K. 1969. Analysis of the seismic coda of local earthquakes as scattered waves, J. Geophys. Res., 74: 615-631.
- Aki, K. and Chouet, B., 1975. Origin of coda waves: source, attenuation, and scattering effects, J. Geophys. Res. 80: 3322-3342.
- Aki, K., 1980. Scattering and attenuation of shear waves in the lithosphere, J. Geophys. Res. 85: 6496-6504.
- Aki K., and Richards P. G., 2002. Quantitative Seismology, Second Edition, University Science Books, Sausalito, CA
- Chouet, B., 1976. Source, scattering, and attenuation effects on high frequency seismic waves, Ph.D. dissertation, Mass. Inst. of Technol., Cambridge, MA.

- Chouet, B. 1979. Temporal variation of earthquake coda near Stone Canyon, California, *Geophys. Res. Lett.*, 6: 143-146.
- Dainty, A. M., 1981. A scattering model to explain seismic Q observations in the lithosphere between 1 and 30 Hz, *Geophys. Res. Lett.*, 8: 1126-1128.
- Dainty, A. M., and Toksöz, M. N., 1977. Elastic wave propagation in a highly scattering medium – A diffusion approach, *J. Geophys.*, 43: 375-388.
- Del Pezzo, E., Bianco, F., Petrosino, S., and Saccorotti, G., 2004. Changes in the coda decay rate and shear-wave splitting parameters associated with seismic swarms at Mt. Vesuvius, Italy, *Bull. Seismol. Soc. Am.*, 94: 439-452.
- Der, Z. A., and Lees, A. C., 1985. Methodologies for estimating $t^*(f)$ from short-period body waves and regional variations of $t^*(f)$ in the United States, *Geophys. J. R. Astr. Soc.*, 82: 125-140.
- Dzurisin, D., Johnson, D. J., Westphal, J. A., 1981. Ground tilts during two recent eruptions of Mount St. Helens, Washington, *Eos, Transactions, American Geophysical Union*, 62 (45): 1089.
- Fehler, M., Roberts, P., and Fairbanks T., 1988. A temporal change in coda wave attenuation observed during an eruption of Mount St. Helens, *J. Geophys. Res.* 93: 4367-4373.
- Fehler, M., Hoshiya, M., Sato, H., and Obara, K., 1992. Separation of scattering and intrinsic attenuation for the Kanto-Tokai region, Japan, using measurements of S-wave energy versus hypocentral distance, *Geophys. J. Int.*, 108: 787-800.
- Gusev, A. A., 1997. Temporal variations of the coda decay rate on Kamchatka: Are they real and precursory? *J. Geophys. Res.*, 102: 8381-8396.

- Jin, A., and Aki, K., 1986. Temporal change in coda Q before the Tangshan earthquake of 1976 and the Haicheng earthquake of 1975, *J. Geophys. Res.*, 91: 665-673.
- Kinoshita, S., 1994. Frequency-dependent attenuation of shear waves in the crust of the southern Kanto area, Japan, *Bull. Seism. Soc. Am.*, 84: 1387-1396.
- Londono, J. M., 1996. Temporal change in coda Q at Nevado Del Ruiz Volcano, Colombia, *J. Volcan. Geotherm. Res.*, 73: 129-139.
- Moncayo, E., Vargas, C., and Durán, J. 2004. Temporal variation of coda- Q at Calderas volcano, Colombia, *Earth Sci. Res. J.*, 8: 19-24.
- Morozov, I. B., 2008. Geometrical attenuation, frequency dependence of Q , and the absorption band problem, *Geophys. J. Int.*, 175: 239-252.
- Morozov, I. B., 2009a. Thirty years of confusion around “scattering Q ”? *Seismol. Res. Lett.*, 80: 5-7.
- Morozov, I. B., 2009b. Reply to “Comment on ‘Thirty Years of Confusion around ‘Scattering Q ’?”” by J. Xie and M. Fehler, *Seismol. Res. Lett.*, 80: 648–649.
- Morozov IB (in press) On the causes of frequency-dependent apparent seismological Q . *Pure Appl. Geophys.*
- Morozov IB (in review) Attenuation coefficients of Rayleigh and Lg waves, *J. Seismol.*
- Morozov, I. B., Zhang, C., Duenow, J. N., Morozova, E.A., and Smithson, S. 2008. Frequency dependence of regional coda Q : Part I. Numerical modeling and an example from Peaceful Nuclear Explosions: *Bull. Seism. Soc. Am.*, 98: 2615–2628, doi: 10.1785/0120080037
- Novelo-Casanova, D. A., Berg, E., Hsu, V., and Helsley C. E., 1985. Time-space variation of seismic S -wave coda attenuation (Q^{-1}) and magnitude distribution (b -

- values), *Geophys. Res. Lett.*, 12: 789-792.
- Novelo-Casanova, D. A., Martinez-Bringas, A., and Valdés-González C., 2006. Temporal variation of Q_c^{-1} and b -values associated to the December 2000 – January 2001 volcanic activity at the Popocatepetl volcano, Mexico, *J. Volcanol. Geotherm. Res.* 152: 347-358.
- Octave, 2009. <http://www.gnu.org/software/octave/about.html> , accessed November 8, 2009.
- Peng, J. Y., Aki, K., Chouet, B., Johnson, P., Lee, W. H. K., Marks, S., Newberry, J. T., Ryall, A., Stewart, S., and Tottingham, D. M., 1986. Temporal change in coda Q associated with the Round Valley, earthquake of November 23, 1984, *J. Geophys. Res.*, 92: 3507-3526.
- Rhea, S. 1984. Q determined from local earthquakes in the South Carolina coastal plain, *Bull. Seismol. Soc. Am.*, 74: 2257-2268.
- Roecker, S. W., Tucker, B., King, J., and Hatzfeld, D. 1982. Estimates of Q in central Asia as a function of frequency and depth using the coda of locally recorded earthquakes., *Bull. Seismol. Soc. Am.*, 72: 129-149.
- Sato, H., 1986. Temporal change of scattering and attenuation associated with the earthquake occurrence – a review of recent studies in coda waves, *Pure Appl. Geoph.*, 126: 465-497.
- Sato, H., 1986. Temporal change in attenuation intensity before and after the eastern Yamanashi earthquake of 1983, in central Japan, *J. Geophys. Res.*, 91: 2049-2061.
- Stewart, R. R., Toksöz, M. N., and Timur A., 1983. Strain dependent attenuation: observation and a proposed mechanism, *J. Geophys. Res.*, 88: 546-554.

Wessel P., and Smith, W. H. F., 1995. New version of the Generic Mapping Tools released:
EOS Trans. Am. Geophys. U., 76: 329.

Figures

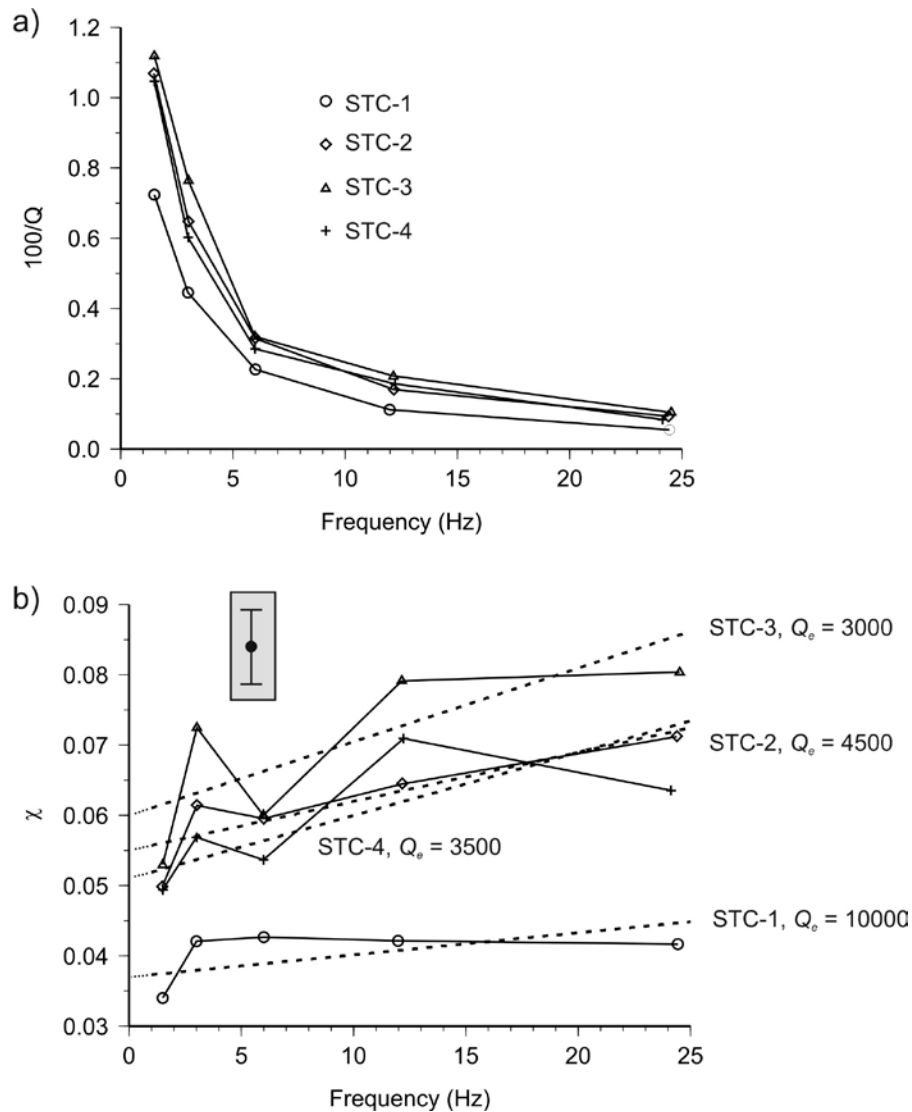


Figure 1. Frequency dependence of local-earthquake coda attenuation at Stone Canyon (California) station from Aki (1980). Labels indicate the consecutive time intervals. a) Data in $100/Q$ form, as in Aki (1980). b) The same data in $\chi(f)$ form. Note that the separation of periods STC-2 through STC-4 is much clearer, and $\chi(f)$ shows linear dependencies on f (dashed lines; Q_e values given in labels). A reference 10% error bar on χ is shown in inset.

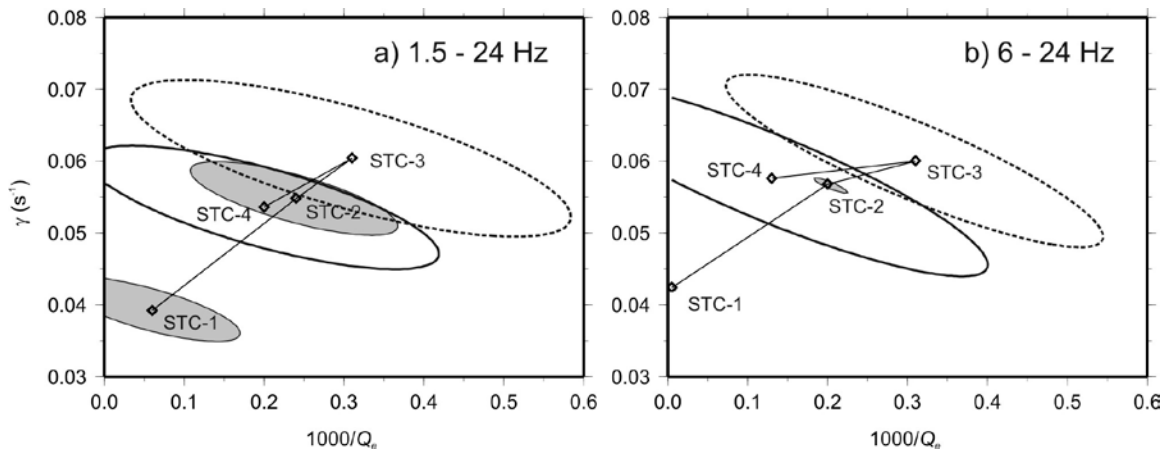


Figure 2. $\gamma - Q_e^{-1}$ cross-plots corresponding to linear $\chi(f)$. Ellipses indicate areas of squared data misfit less than twice higher than for the optimal (γ, Q_e) values (diamonds). a) Fitting using the entire 1.5 – 24 Hz frequency band; b) using frequencies 6 – 24 Hz. Note the temporal trends in both γ and Q_e (lines).

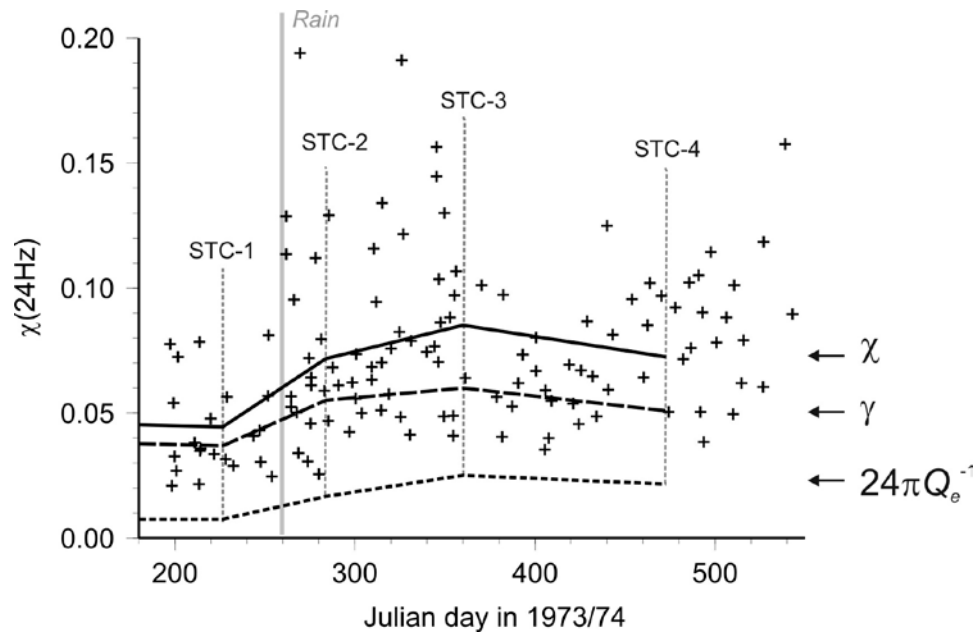


Figure 3. Temporal variations of local-coda χ in Stone Canyon at 24 Hz. Crosses are coda data from Chouet (1979), and black lines show the interpreted γ values (dashed), contribution from Q_e^{-1} (short dash), and total χ (solid) from Figure 1. Grey lines indicate middles of measurement intervals (dashed) and the start of rain season (October 7, 1973; Aki, 1980).

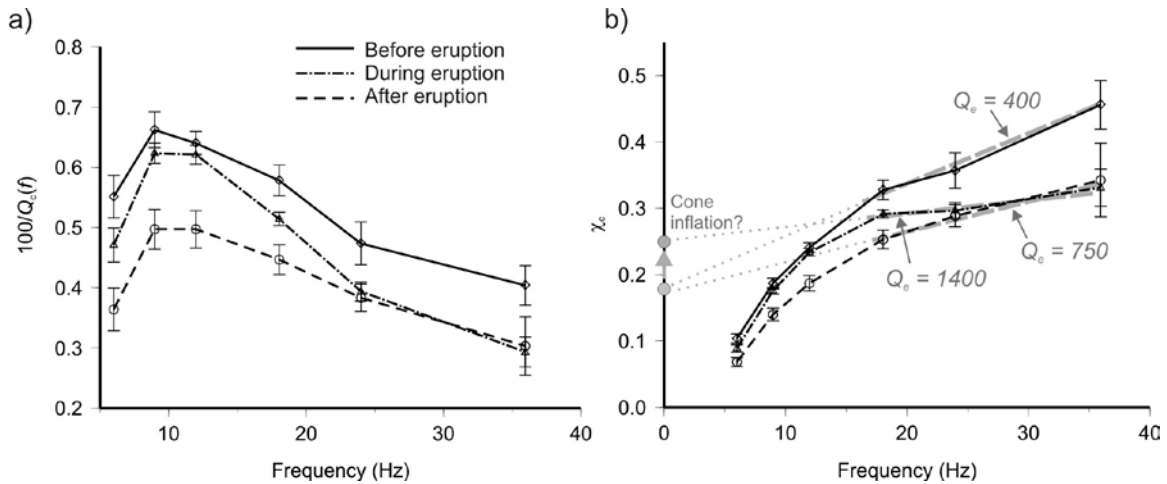


Figure 4. Coda attenuation data at Mount St. Helens. a) $Q_c^{-1}(f)$ data (Fehler et al., 1988).

Note the peak at 10 Hz and decreasing Q_c^{-1} after the eruption. b) The same data in $\chi_c(f)$ form. Dashed grey lines show the interpreted linear trends in $\chi_c(f)$. Note the linear $\chi_c(f)$ dependences at $f > \sim 18$ Hz, with slope decreasing after the eruption.